Zifan, A., Liatsis, P., Kantartzis, P., Gavaises, M., Karcanias, N. & Katritsis, D. G. (2008). Automatic 3D Reconstruction of Coronary Artery Centerlines from Monoplane X-ray Angiogram Images. International Journal of Biological and Medical Sciences, 2(3), pp. 105-110.

CITY UNIVERSITY LONDON

EST 1894

[City Research Online](#)

Automatic 3D Reconstruction of Coronary Artery Centerlines from Monoplane X-ray Angiogram Images

Ali Zifan [1], Panos Liatsis [1], Panagiotis Kantartzis [1],
Manolis Gavaises [1], Nicos Karcanias [1], Demosthenes Katritsis [2]

Abstract—We present a new method for the fully automatic 3D reconstruction of the coronary artery centerlines, using two X-ray angiogram projection images from a single rotating monoplane acquisition system. During the first stage, the input images are smoothed using curve evolution techniques. Next, a simple yet efficient multiscale method, based on the information of the Hessian matrix, for the enhancement of the vascular structure is introduced. Hysteresis thresholding using different image quantiles, is used to threshold the arteries. This stage is followed by a thinning procedure to extract the centerlines. The resulting skeleton image is then pruned using morphological and pattern recognition techniques to remove non-vessel like structures. Finally, edge-based stereo correspondence is solved using a parallel evolutionary optimization method based on f symbiosis. The detected 2D centerlines combined with disparity map information allow the reconstruction of the 3D vessel centerlines. The proposed method has been evaluated on patient data sets for evaluation purposes.

Keywords—Vessel enhancement, centerline extraction, symbiotic reconstruction.

I. INTRODUCTION

CORONARY X-ray angiography is performed to specifically image and diagnose diseases of the blood vessels of the heart. A major component of any coronary analysis tool is the accurate estimation of the vessel centerlines. The extraction of vessel centerlines allows for better understanding of their topology, and can be used in computing the optimal orientation of the imager for stenosis characterization [1] or to give an initial point for the computation of the deformation field of the vessels along the cardiac cycle [2], [3]. Currently, no standard tool is available for extracting the centerlines. We describe an automatic system for constructing 3D models of the coronary artery centerlines from single – plane angiograms. Monoplane angiography provides fast information on the vascular system and allows the physicians to surgically interact during the image acquisition phase, thus making it the most common approach when it comes to diagnosis, planning and execution of different cardiovascular treatment methods. Previous work in this field is mainly based on semi-automatic methods for the detection and segmentation of the arterial tree and is limited to in-vitro bi-plane angiograms [4-8], although an automatic approach using monoplane angiograms has also been proposed [9](see also [10] for a review of different approaches in the literature).

In this paper a new vessel enhancement method, based on a multi-scale approach is presented. Moreover, morphological operations, and pattern recognition and evolutionary techniques will serve as a means to extract and reconstruct the complete arterial tree centerline from X-ray angiogram images. In the next section, we will describe in detail the steps involved.

II. METHODOLOGY

A. Image Acquisition

For all procedures a Philips Integris 3000H X-Ray C-arm unit was used with an under couch tube/over couch image intensifier configuration. The gantry performs a rotation while acquiring the images [11]. The gantry motion is characterized by constant SID (Source Intensifier Distance) value, constant CRA/CAU (Cranio/Caudal) angle value, and varying LAO/RAO (Left/Right Anterior Oblique) angle. The rotational acquisition is performed with a zero Cranial/Caudal angle and with the Left Anterior Oblique (LAO)/Right Anterior Oblique (RAO) angle varying from 90 degrees RAO to 90 degrees LAO. Two images of the same cardiac phase are selected from the angiogram sequence. The best projections obtained were along left anterior oblique (LAO), 30° LAO caudal, 30° LAO cranial, anteroposterior with cranial and caudal angulation, right anterior oblique (RAO), 30° RAO caudal, and 30° RAO cranial and left lateral. Pulsed fluoroscopy (12.5 p/s) was used. The process is ECG gated thus we can determine the phase of heart beat for each frame. Gantry information including focal spot to image intensifier
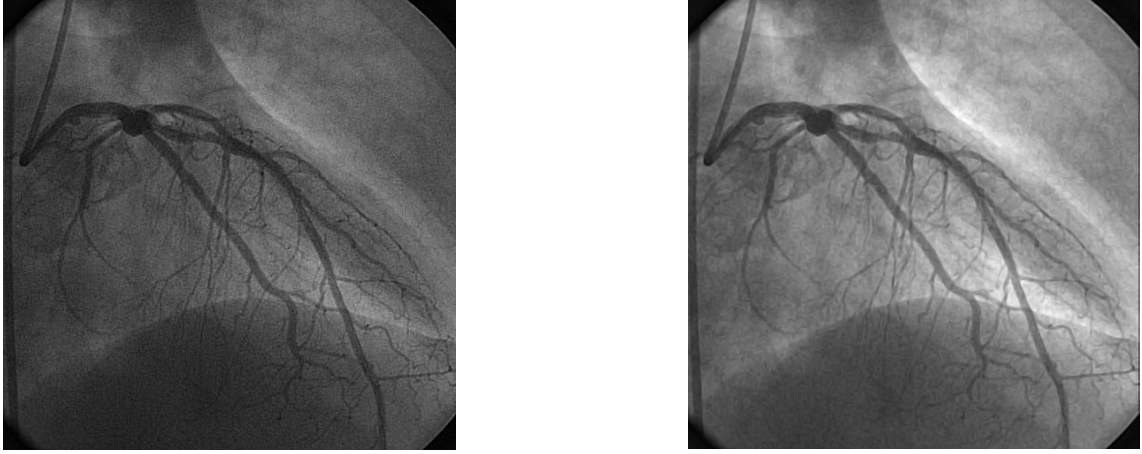
Fig. 1 Result of smoothing on one of the angiogram images: (Left) Original X-ray image (Right) Corresponding smoothed image

distance (SID), field of view (FOV) and gantry orientation were automatically recorded and stored with each image file. All procedures were performed in accordance with institutional guidelines, and all patients gave informed consent before PCI. For each patient, we have a single rotational sequence consisting of 40-50 images with pixel resolution of 512×512 and pixel size of 0.2 mm. In addition, a precalibration step allows the estimation of the geometrical acquisition parameters.

B. Smoothing

First the input images are normalized. Then, their content is regarded as a compilation of iso-intensity contours. Spikes of noise corresponding to high curvature are removed and oscillations in boundaries smoothed out using variations of curvature flow [12]. The curvature evolution equation is as follows:

$$k = \nabla \cdot \frac{\nabla I}{|\nabla I|} \tag{1}$$

The goal is to generate a flow, which will smooth out undesired oscillations yet maintain fundamental characteristics of the shape. The concept of min/max switch is utilized in the following function:

$$\bar{F}_{min/max} = \begin{cases} \max(k,0) & if \ Ave_{\phi(x,y)}^{R=kh} < T_{threshold} \\ \min(k,0) & otherwise \end{cases} \tag{2}$$

Finally, $I_t = -\bar{F}|\nabla I|$.

The Ave function is the average value of ϕ, given a disk of radius $R = kh$ centered on a point $(x; y)$. k is chosen as 1, a choice which allows some movement of the zero level corresponding to the boundary [12]. Finally, a speed function dependent on the average value of f and the local level of curvature is obtained. Given $I(x; y)$, the original intensity

profile, one iterates until I_t goes to zero and stable values are reached. The results of the smoothing are shown in Figure 1.

C. Proposed Vessel Enhancement Method

In X-ray angiography, blood vessels often exhibit low intensity contrast with respect to their surrounding soft tissues. The problem is particularly severe for fine vessel structures. A major challenge for enhancement is the ability to emphasize vessel structures without creating artifacts such as edge overshot and noise magnification. Ideally, vessel enhancement filters should enhance vessels and vessel junctions, while suppressing nodules and other non-vessel elements.

Digital subtraction angiography (DSA) [13] is a common approach to suppress these problems. However, DSA works well only on static areas with no ongoing motion (such as the vascular system of the brain). In cardiac angiography the heart muscle constantly moves and a DSA approach creates motion artefacts which could be confused with vessels.

A common approach to analyze the local behavior of a 2D/3D image I is to consider its Taylor expansion in the neighborhood of a point x_0

$$I(x_0 + \Delta x) \approx I(x_0) + \Delta x^T \nabla I(x_0) + \Delta x^T H(x_0) \Delta x \tag{3}$$

where ∇I is the gradient vector and H denotes the Hessian matrix – the matrix of the second-order partial derivatives of I.

$$H = \begin{pmatrix} I_{xx} & I_{xy} \\ I_{yx} & I_{yy} \end{pmatrix} \tag{4}$$

where $I_{ab} = \dfrac{\partial^2 I}{\partial a \partial b}$ is the Hessian matrix for a 2D image.

The elements of the Hessian matrix approximate the 2nd order derivatives, and therefore encode the shape information

– both a qualitative and quantitative description of how the normal to an isosurface changes. Particularly interesting are the eigenvalues and eigenvectors of the Hessian matrix. Sato et al. [14] and Frangi et al. [15] independently employ eigenvalues to design filters for vessel enhancement in 3D medical digital images.

In this paper, we propose a simple yet highly efficient way to enhance vessels in 2D images. The method is described as follows:

First a multi-scale representation of the input image is obtained over 8 exponentially distributed scales in the interval [0.8, 8] mm (note: scale normalization is achieved by multiplying the Hessian matrix by σ^2 before eigenvalue decomposition, where σ is the scale for calculating Gaussian image derivatives). Next, we calculate 2nd-order derivatives of each image build the Hessian matrix H for every pixel in each image and decompose it into its corresponding eigenvalues λ_1, λ_2 where $|\lambda_2| \gg |\lambda_1|$ for a bright structure on a dark background. Hence, for every pixel in each image, there will be two eigenvalues. This procedure is performed for all 8 scales. During each step, we store the $|\lambda_2|/\sqrt{\lambda_1^2 + \lambda_2^2}$ ratio value for each pixel and after a whole run on a certain scale, the sum of these ratios (i.e., $\sum \left|\lambda_{2(i,j)}/\sqrt{\lambda_{1(i,j)} + \lambda_{2(i,j)}}\right|$ where i and j are the pixel coordinates) is computed over all the rows and columns of the image. We call this number, the winner factor (WF) (note that if for a scale, we have $\lambda_1 = \lambda_2 = 0$, we ignore that scale to avoid any division by zero.)

Finally, having performed the same process on all the other scales, we find the winner image (WI) by comparing their respective winner factors. The scale with the largest WF is chosen as the winner with the strongest response and the last 4 scales with low scores are removed. Next, for each pixel in the WI a search is done pixel-by-pixel to compare the $|\lambda_2|/\sqrt{\lambda_1^2 + \lambda_2^2}$ ratio of the WI pixels with those of the 4 remaining scales. If there exists any scale with a
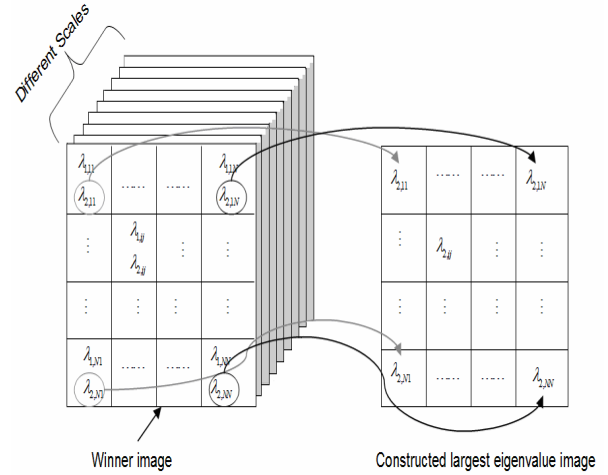

Fig. 2 Visual illustration of eigenvalue selection procedure

higher ratio at the same pixel location, then the eigenvalues of the WI at that pixel location are substituted with the ones of the other scale with the higher ratio.

Following this, we initialize a new blank image with the same size as the WI. The pixel values of this new image will be the corresponding largest eigenvalues of the modified winner image in the same pixel coordinates. This procedure can be better understood through Figure 2.

In Figure 3(Left) we can observe the application of the above procedure to one of the X-ray images in the database. Finally, in order to obtain the vessel enhanced image, this new image is multiplied element-wise with itself to get the final enhanced vessels. The result of the enhancement stage is shown in Figure 3(Right) for the same X-ray angiogram image.

Region growing approaches [16], [17] and parametric deformable models (snakes) [18] are methods commonly used for vessel extraction. The main disadvantage of these
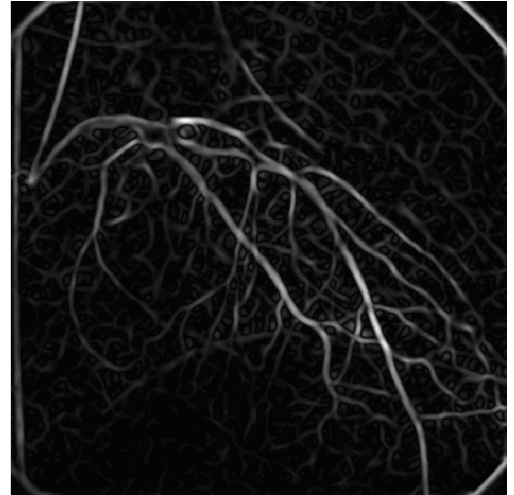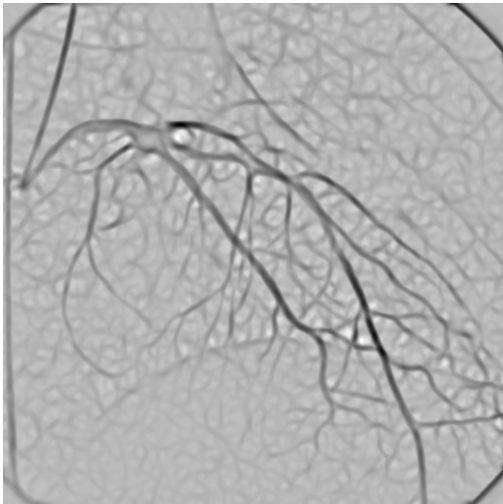

Fig. 3 (Left) Max Eigenvalue image   (Right) Vessel enhanced using the proposed method

approaches is that they often require user interaction in form of manually defined seed points, thus making it quite time consuming. A method that binarizes the vessel enhanced image, using hysteresis thresholding [19] followed by a thinning procedure [20], to extract the arterial centrelines, is considered next in this paper. The thinning procedure reduces the amount of data and shape analysis can be more easily made. Vessel bifurcations and end points are automatically extracted and organized into a tree structure that makes it easy to find specific parts of the coronary tree.

D. Hysteresis-like Thresholding

Hysteresis thresholding is suited to discard non-tubular structures since it offers the possibility to retain only the elements that match both an intensity criterion and a criterion of size of the connected components. Firstly, we choose a high threshold to recognize tubular complexes. Secondly, we choose a low threshold with which only the brighter parts of tubule complexes are recognized as foreground (since we use the negatives of the images). The threshold values are chosen low enough to obtain a light over-segmentation. We compute these thresholds as quantiles of the histogram of the vessel enhanced image. These quantiles are associated to the relative area occupied by vessels in the image. From our experiments, we chose the 93rd percentile for the low threshold and the 98th percentile for the high threshold.

E. Extracting Vessel Centerlines

An important observation is that the vessel enhancement procedure described in section C produces a low vesselness response to blob-like structures. Structures in the image with similar properties as the blob-like structures are the vessel bifurcations. Hence, bifurcations will give a lower vesselness response than an ordinary vessel segment. The low response can produce small holes in the binarized image, although they may seem harmless however the thinning algorithm will expand the holes and produce additional lines and bifurcation points not reflecting the structure of the vessel tree. Hence, a morphological 'closing' operator is applied prior to thinning in order to remove these additional lines.

The aim of skeletonization is to extract a region-based shape feature representing the general form of an object, in our case the vessel. In this stage, the skeleton is obtained using the thinning method proposed in [20]. Here, we want to produce a clean and complete vascular tree structure by removing isolated artifacts and pixels. Hence, the next step is to build a tree structure describing the vessel tree. This includes finding bifurcation points, end points.

- *Finding intersecting and end points:*

The bifurcation detection algorithm uses a 3×3 window to scan the image looking for patterns shown in Figure 4. Notice that these patterns are just four examples of the segment types. By rotating these patterns 45 degrees or by changing the binary value of a pixel, all possible patterns can be found.

For extracting the endpoints, consider a point on the centerline (or any pixel in the binarized thinned image), and assume that a minimum radius circle has been drawn from each point of the skeleton which has at least one point common with a region boundary. Let contact be each contiguous subset of the circle which is common to the circle and to the boundary. If a circle drawn from its center (say K) has one contact only, then K is a skeleton endpoint. If the point K has two contacts, it is a normal skeleton point. If K has three or more contacts, the point will be a skeleton node-point. The result of the bifurcation and endpoint detection for the right hand side image of figure is shown in figure 4.

The resulting detected bifurcation and endpoints are shown in Figure 5. Finally for the complete extraction of the tree, first pixels between two endpoints without any bifurcation in between are removed. Next, Size filtering is used to remove isolated pixels or regions that are not part of the arterial tree, by using the concept of connected pixels labeling. Connected regions correspond to individual objects. We first need to identify separate connected regions. Area filtering tries to isolate the individual objects by using the information of a eight-connected neighborhood and label propagation. Once the algorithm is completed, only the resulting classes exceeding a certain number of pixels are labeled as blood vessels.
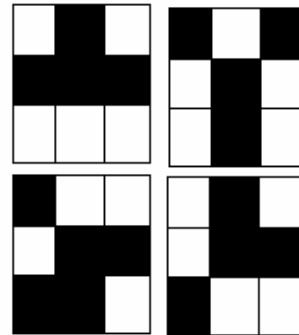

Fig. 4 patterns used for detecting bifurcations

F. 3D Centerline Reconstruction

Centerline reconstruction allows the estimation of the magnification factor attached to a 2-D point (at a reference time), which yields better measurements, as well as optimal viewing angles to avoid overlapping and vessel shortening [21], [22]. For reconstructing the centerlines in 3D, we make use of a feature-based symbiotic genetic optimization scheme capable of optimizing both intra- and inter-row levels simultaneously [23]. It utilizes symbiotic Genetic Algorithms, which are based on the biological paradigm of symbiosis and work on different subparts of a decomposable large-scale intractable problem.
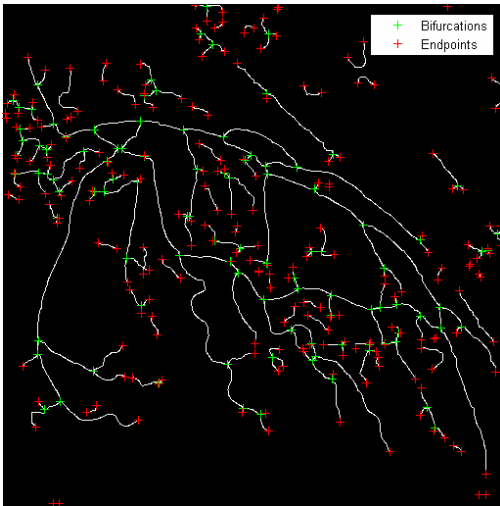
Fig. 5 detected bifurcation and endpoints

The populations interact through the fitness evaluation function and affect each other continuously, towards the cooperative solution of the large-scale problem. This allows accurate disparity calculations by performing matching of low-level primitives (edgels), while using composite higher-level structures (edge chains) to maximize Figural Continuity. Inter-row consistency is enforced in a powerful way along edge chains of variable shapes and lengths. Unlike DP-based approaches, intra-row search is not restricted by the ordering constraint. A robust match functional based on fuzzy set theory is used to combine the feature attributes and for measuring the probability of matching two individual edgels. Using the above approach we obtain the disparity map as shown in the middle image of Figure 6.

III. RESULTS

We applied the proposed algorithm to a database, which was provided by the Athens Euroclinic medical center, acquired from patients who held their breath during each acquisition.

It should be noted that the reconstruction of patient's data is more challenging, and is also more difficult to assess. We show the extracted centerlines along the corresponding disparity map from for a pair of two left and right images in Figure 6. The detected 2D centerlines combined with disparity map information will allow the reconstruction of the 3D vessel centerline*s*. The typical running time of our centerline extraction system on a 3.20GHz Pentium IV is 25.8 seconds on average for an 512×512 X-ray angiogram image.

IV. CONCLUSION

We described a new method for the 3D reconstruction of coronary artery centerlines from X-ray angiogram images obtained from one single rotational acquisition. The images are enhanced, in a multi-scale manner, by convolution with the second order derivative of a Gaussian kernel at different sizes. The proposed vessel enhancement procedure shows excellent background and noise suppression results, when applied to the angiograms. To extract the vessel centrelines, a thinning method is applied. By extracting corresponding feature points in the X-ray images and combining it with a priori information about the scene, it is possible to estimate the epipolar geometry and reconstruct the scene in three dimensions. The results obtained so far demonstrate the feasibility of the proposed approach. The final as well as the intermediate results have the potential to support image interpretation and quantification by the physician. After clinical validation, this model could be used to help diagnose cardiovascular diseases. Further research in the area includes the evaluation of the effect of vessel geometry as well as stenosis geometry on the flow within the vessel and also the detection of thin and low-contrast vessels while avoiding false detection of vessels near pathologies and other non-vascular structures.
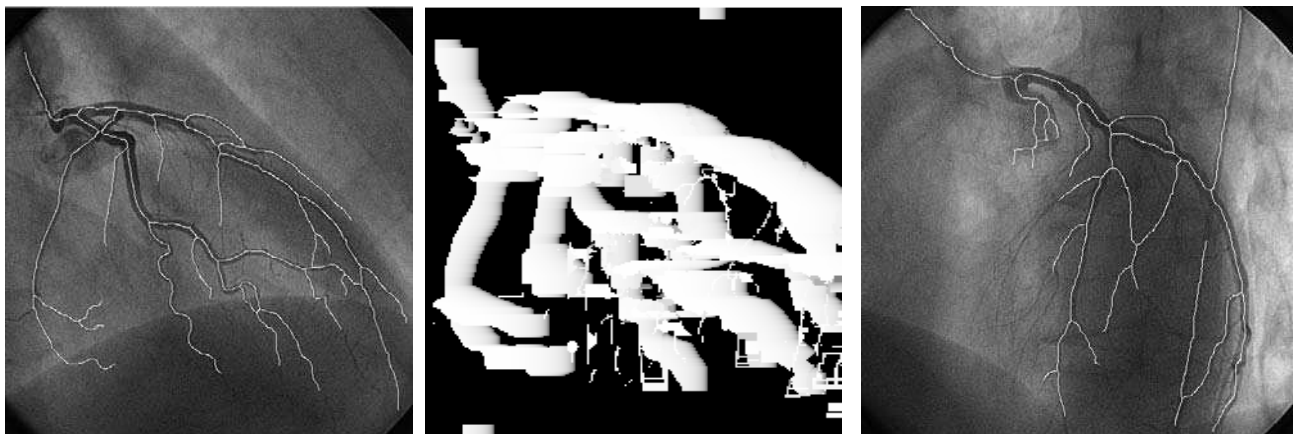

Fig. 6 Left & Right: Angiogram image with superimposed extracted centelrines. Middle: The computed disparity map sing symbiosis.

REFERENCES

[1] Chen S.Y. and Carroll J.D. Computer Assisted Coronary Intervention by Use of On-line 3D Reconstruction and Optimal View Strategy. Medical Image Computing and Computer-Assisted Intervention Proceedings, Lecture Notes in Computer Science Vol. 1496: 377-385, Springer, Cambridge, October 1998.

[2] Shechter G., Devernay F., Coste-Manière E. and McVeigh E. Temporal tracking of 3D coronary arteries in projection angiograms. Proceedings of SPIE Medical Imaging 4684, San Diego, February 2002.

[3] Ding Z. and Friedman M.H. Quantification of 3-D coronary arterial motion using clinical biplane cineangiograms. The International Journal of Cardiac Imaging 16(5): 331-346, October 2000.

[4] Chen S.Y. and Carroll J.D. 3-D reconstruction of coronary arterial tree to optimize angiographic visualization. IEEE Transactions in Medical Imaging 19(4), April 2000.

[5] S. Ruan, Bruno A., and J. Coatrieux. Three-dimensional motion and reconstruction of coronary arteries from biplane cineangiography. Image and Vision Computing, 12(10):683–689, dec. 1994.

[6] T. Sato, M. Araki, H. Hanayama, H. Naito, and S. Tamura. A viewpoint determination system for stenosis diagnosis and quantification in coronary angiographic image acquisition. IEEE Trans. medical imaging, 17(1), 1998.

[7] A. Wahle, H. Oswald, and E. Fleck. 3d heart-vessel reconstruction from biplane angiograms. IEEE Computer Graphics and Applications, 16:65–73, jan. 1990.

[8] P.Windiga, M. Garreau, and J. Coatrieux. Estimation of search-space in 3d coronary artery reconstruction using biplane images. Pattern Recognition Letters, 19:1325–1330, sept 1998.

[9] C. Blondel, R. Vaillant, F. Devernay, G. Malandain, and N. Ayache Automatic Trinocular 3D Reconstruction of Coronary Artery Centerlines from Rotational X-ray Angiography Proceedings of Computer Assisted Radiology and Surgery(CARS)Paris, June 2002. Springer Publishers, Heidelberg.

[10] C. Kirbas and F. Quek. A review of vessel extraction techniques and algorithms. ACM Computing Surveys, 36(2):81–121, 2004.

[11] S. V. Raman, R. Morford, M. Neff, T. T. Attar, G. Kukielka, R. D. Magorien, and C. A. Bush, "Rotational X-ray coronary angiography," *Catheterization and Cardiovascular Interventions*, vol. 63, no. 2, pp. 201–7, 2004.

[12] J.A. Sethian. Fast Marching Methods and Level Set Methods: Evolving Interfaces in Computational Geometry, Fluid Mechanics, Computer Vision and Materials Sciences. Cambridge University Press, 1999.

[13] W. R. Brody. *Digital Radiology*, volume vol. I+II. Raven Press, 1984.

[14] Yoshinobu Sato, Carl-Fredrik Westin, Abhir Bhalerao, Shin Nakajima, Nobuyuki Shiraga, Shinichi Tamura, and Ron Kikinis. Tissue classification based on 3D local intensity structures for volume rendering. IEEE Transactions on Visualization and Computer Graphics, 6(2):160–180, 2000.

[15] A. F. Frangi, W. J. Niessen, K. L. Vincken, and M. A. Viergever. Multiscale vessel enhancement filtering. Lecture Notes in Computer Science, 1496:130–137, 1998.

[16] J. F. OBrien and N. F. Ezquerra. Automated segmentation of coronary vessels in angiographic image sequences utilizing temporal, spatial structural constraints. Proc. SPIE Conf. Visualization in Biomed. Computing, 1994.

[17] H. Schmitt, M. Grass, V. Rasche, O. Schramm, S. Haehnel, and K. Sartor. An x-ray-based method for the determination of the contrast agent propagation in 3-D vessel structures. IEEE Trans. medical imaging, 21:251–262, march 2002.

[18] M. Kass, A. Witkin, and D. Terzoopoulos. Snakes: Active contour models. Int. Journal of Computer Vision, pages 321–331, 1988.

[19] J. F. Canny. Finding edges and lines in images. Technical Report 720, MITAIL, 1983.

[20] Patrick Shen-Pei Wang, Edward Y. Y. Zhang: A Fast and Flexible Thinning Algorithm. IEEE Transactions on Computers 38(5): 741-745, 1989.

[21] O. Wink, R. Kemkers, S.-Y. J. Chen, S. Chen, and J. D. Carroll. Intraprocedural coronary intervention planning using hybrid 3-dimensional reconstruction techniques. Academic Radiology, vol. 10, no. 12, pp. 1433–41, 2003.

[22] T. Sato, T. Araki, and M. Hanayama. A viewpoint determination system for stenosis diagnosis and quantification in coronary angiographic image acquisition. IEEE Transactions on Medical Imaging, vol. 17, no. 1, pp. 121–137, 1998.

[23] J.Y. Goulermas and P. Liatsis, "Hybrid symbiotic genetic optimization for robust edge-based stereo correspondence", Pattern Recognition, Vol. 34, pp. 2477-2496, 2001